Multifractals embedded in short time series: An unbiased estimation of probability moment

Lu Qiu,[1] Tianguang Yang,[2] Yanhua Yin,[1] Changgui Gu,[1] and Huijie Yang[1,*]

[1]*Business School, University of Shanghai for Science and Technology, Shanghai 200093, China*

[2]*Department of Statistics, School of Mathematical Sciences, Nankai University, Tianjin 300071, China*

(Received 31 January 2016; revised manuscript received 23 September 2016; published 1 December 2016)

An exact estimation of probability moments is the base for several essential concepts, such as the multifractals, the Tsallis entropy, and the transfer entropy. By means of approximation theory we propose a new method called factorial-moment-based estimation of probability moments. Theoretical prediction and computational results show that it can provide us an unbiased estimation of the probability moments of continuous order. Calculations on probability redistribution model verify that it can extract exactly multifractal behaviors from several hundred recordings. Its powerfulness in monitoring evolution of scaling behaviors is exemplified by two empirical cases, i.e., the gait time series for fast, normal, and slow trials of a healthy volunteer, and the closing price series for Shanghai stock market. By using short time series with several hundred lengths, a comparison with the well-established tools displays significant advantages of its performance over the other methods. The factorial-moment-based estimation can evaluate correctly the scaling behaviors in a scale range about three generations wider than the multifractal detrended fluctuation analysis and the basic estimation. The estimation of partition function given by the wavelet transform modulus maxima has unacceptable fluctuations. Besides the scaling invariance focused in the present paper, the proposed factorial moment of continuous order can find its various uses, such as finding nonextensive behaviors of a complex system and reconstructing the causality relationship network between elements of a complex system.

DOI: 10.1103/PhysRevE.94.062201

I. INTRODUCTION

A stochastic process can be described with probability distribution function (PDF) of its displacement x at time t, denoted with $p(x,t)$. The process behaves multifractal, providing the partition function obeys [1]

$$z(t,q) \equiv \int_{-\infty}^{+\infty} p^q(x,t)dx \sim t^{-\tau(q)}, \tag{1}$$

where $q \in (-\infty, +\infty)$ is used to extract different components of $p(x,t)$ that are scaling-invariant with exponents $\tau(q)$, respectively.

From a stationary time series, one can extract all the possible segments with a predefined length s. Regarding each segment as a trajectory of a stochastic process, all the trajectories (segments) are accordingly a bundle of realizations of the process, which form an ensemble. From all the displacements of the realizations one can obtain the probability distribution function $p(x,s)$. If $p(x,s)$ obeys the power-laws in Eq. (1), the time series is called to behave multifractal [2–8].

Multifractal embedded in time series finds its great use in diverse research fields (see [9–12] and the references therein for important contributions in this field). For instance, a large amount of time series in financial markets behave multifractal [13–27], based upon which the fractal market theory is established to replace the efficient market hypothesis [28]; multifractals embedded in physiological signals provide us helpful information on healthy states [29–38]; along a DNA sequence, some regions guide the production of proteins, while some other regions take part in the regulation of protein production. In the coding regions the base pairs are positioned randomly, and in the noncoding regions the base pairs distribute according to (multi)fractal [39–42]. This fact is widely used to distinguish coding regions from noncoding regions in DNA sequences [41,42].

Precise estimation of the partition function requires an infinite (at least a large enough) number of segments, namely, infinite length of the considered time series. However, in reality we have only time series containing a finite number of records. Sometimes monitoring dynamical process of a complex system produces a long time series, but in the time duration structure of the system may have changed significantly, or the dynamical process has transited to other attractors. We should separate the long series into parts to obtain evolutionary behaviors of the system. Finite length of time series may lead to unacceptable fluctuation to the probability $p(x,s)$ and subsequently serious statistical fluctuation and bias to the term $p^q(x,s)$ in the partition function, a nonlinear function of the probability ([43]; see also the Sec. II for detail). How to detect exactly multifractals from real-world time series is still an open problem.

Actually, almost all the standard tools widely used to evaluate scaling-invariance require the length of a time series being infinite or large enough. Extensive calculations show that [44–49], to obtain reliable scaling behaviors of a time series, the length should reach 2^{13} and 2^{15} for wavelet analysis [29,50] and detrended fluctuation analysis [51–55], respectively. For the R/S method [56], even a length of 2^{16} cannot provide us a well-converged result. Very recently, Bonachela *et al.* proposed a balanced estimation of entropy to minimize the summation of bias and statistical fluctuation [57]. This concept performs well even for small sets of data containing few tens of records. Replacing the original Shannon entropy with this new estimation, we convert the diffusion entropy approach [2–4,58–74] [a novel method to evaluate the scaling exponent

*hjyang@ustc.edu.cn

$\tau(q \to 1)$] to a new version, called balanced estimation of diffusion entropy [75–78], by which one can obtain reliable values of $\tau(q \to 1)$ for very short time series with several hundred lengths. But this new version of diffusion entropy can only evaluate monofractals.

In the research branch of high-energy collision, a critical problem is how to uncover dynamical behaviors covered by large statistical fluctuations due to a limited number of experiments. An important concept called factorial moment [79–88] is proposed to extract intermittency (multifractal) behaviors from several tens of experimental cases. From the experimental cases, one can find the distribution region of measured quantities. Separating the region into many bins and reckoning the number of particles occurring in each bin. In the rth experimental case the number of particles occurring in the jth bin is here denoted with $n_r(j,s)$, where s is the size of a bin. A basic estimation of the occurring probability in this bin is $n_r(j,s)$ over the total number of particles. And the partition function is subsequently estimated to be proportional to the summation of the moments $n_r^q(j,s), j = 1,2,\ldots,J$. J is the number of the bins. The key idea of factorial moment is to replace the moment $n_r^q(j,s)$ with a factorial moment $n_r(j,s)[n_r(j,s)-1][n_r(j,s)-2]\ldots[n_r(j,s)-q+1]$.

A large amount of works prove the powerfulness of factorial moment in filtering out large fluctuations and subsequent bias induced by Poisson noise (see, for examples, Refs. [41,83–92]. It can expose exactly dynamical behaviors of a complex system. But this solution is valid only for positive integer values of q. Hwa [93] extends the idea to real values of q by taking an expansion of the distribution of $n(j,s), j = 1,2,\ldots,J$ in terms of negative binomial distributions. But the procedure requires exact coincidence of the expansion with experimental data, which leads to unreasonably large (absolute) and alternatively occurring positive and negative values of the set of fitting parameters [94].

In the present paper, starting from the idea of factorial moment, by using the approximation theory of functions we extend the original definition of factorial moments to a version of continuous order, which makes it possible to estimate exactly the partition function (without bias) and subsequent multifractal behaviors for very short time series. The contribution is multifold,

First, we introduce the basic and the integer-order factorial-moment-based estimations of partition function. Their performances are measured by the theoretical predictions of biases and fluctuations, which are verified also by detailed calculations, respectively.

Second, an unbiased estimation of partition function, a new concept called continuous q-order factorial moment, is developed to evaluate scaling behaviors embedded in short time series. A probability moment is approximated with a polynomial function of probability, by use of which the continuous q-order partition function is transformed to a summation of positive-integer-order factorial moments. Performance of this solution is shown as a typical example by measuring exactly the multifractal structure in the probability redistribution model.

Third, we investigate the evolutionary behaviors of two empirical records. The first case contains three walking trials (fast, normal, and slow) for a healthy volunteer. From the gait time series we extract five successive nonoverlapping segments with a length of 500 each. It is found that all the segments display perfect multifractal behaviors. The multifractal strength for the fast trivial changes abruptly, while that for the normal and slow trials behave similar with each other. As the second example, the Shanghai stock market index series in the duration from 1995 to 2015 is separated into seven periods covering three years each. All the periods have large multifractal strengths. Interestingly, in the period of 2007–2009, which covers the famous global financial crisis occurring in the year 2008, the multifractal strength is the weakest, while that for the successive duration of 2010–2012 is the strongest, which is regarded here as the relaxation from abnormal to normal state. The durations of 2004–2006 (before the global crisis) and 1998–2000 (after the Asia financial crisis occurring in the year 1997) behave very similar to that for the extreme case in the duration of 2007–2009, all of which form a crisis-cluster. The other durations far from the crises behave very similar to each other and form a distinguished normal-cluster.

Fourth, as a comparison, the well-established tools to evaluate multifractals, such as the basic estimation of partition function, the multifractal detrended fluctuation analysis (MF-DFA), and the wavelet transformation modulus maxima (WTMM), are also used to detect the scaling behaviors in the empirical data. With the increase of scale the basic estimation of partition functions [see Eq. (5) in Sec. II for detail] bends down significantly. The MF-DFA method, on the contrary, fails in the small scales. The estimations using the WTMM have unacceptable large fluctuations in all the considered scales. The continuous q-order factorial moment proposed in this paper can estimate the partition functions perfectly in a wide range of scale and evaluate reliably multifractals in very short time series. This conclusion is also confirmed by using a large amount of fractional Brownian motions.

It should be emphasized that the key contribution of the present work is an unbiased estimation of the probability moments of continuous order. Besides its application in evaluating scaling invariance embedded in short time series as being focused on in this paper, it can be extended straightforwardly to estimate entropies defined with various formulas. For instance, the Tsallis entropy [95–97] can be estimated with $\frac{1-z(t,q)}{1-q}$, which shows us the nonextensive behaviors of a complex system. It can also be used to estimate transfer entropy between each pair of elements of a complex system, based upon which one can find causalities and reconstruct subsequently a relationship network between the elements [98,99].

In Sec. II we introduce the basic estimation of multifractals (Sec. II A), and then develop a new method called factorial-moment (FM)-based estimation of partition functions (Secs. II B and II C). Performance of each method is measured by the average and the variance. A remark on the algorithm of the FM-based estimation is presented (Sec. II D). Several well-established tools to evaluate scaling behaviors of time series are introduced finally for comparison (Sec. II E). In Sec. III materials are introduced in detail, including the probability redistribution model by which one can generate a perfect multifractal structure and its realizations (Sec. III A), the stride interval series of gait trials for a healthy volunteer as the first empirical case (Sec. III B), and the closing price series of the Shanghai Stock Market as the second empirical case (Sec. III C). In Sec. IV the theoretical predictions of performance are verified by calculations (Secs. IV A and IV B), and the FM-based estimation is used to find the evolutionary behaviors in the two empirical cases (Secs. IV C and IV D). A detailed comparison with the well-established tools is presented in Sec. IV E. We finish with concluding remarks in Sec. V.

II. METHOD AND MATERIALS

A. Basic evaluation of multifractals in time series

Let us start from a stationary time series, $\xi = \{\xi_1,\xi_2,\ldots,\xi_N\}$. All the possible segments with length s read

$$X_i^s = \{\xi_i,\xi_{i+1},\ldots,\xi_{i+s-1}\}, \quad i = 1,2,\ldots,N-s+1. \quad (2)$$

Now we regard X_i^s as a realization of a stochastic process, namely, the trajectory of a particle walking randomly from the original point in one-dimensional space [4]. The duration is a total of s time units. All the $N-s+1$ realizations form an ensemble, displacements of which read,

$$x_i(s) \equiv \sum_{j=1}^{s} X_i^s(j) = \sum_{j=i}^{i+s-1} \xi_j, \quad i = 1,2,\ldots,N-s+1. \quad (3)$$

Selecting a certain fraction of the standard deviation of the initial time series as the size of a bin, i.e., $\frac{1}{\epsilon}\sqrt{\sum_{j=1}^{N}(\xi_j - \langle\xi\rangle)^2}$ (for instance, $\epsilon = 2$) [4], one can separate the distributing region of displacement into many bins, denoted with $K(s)$, where $\langle . \rangle$ is the average. Reckoning the number of displacements occurring in every bin, denoted with $n(k,s), k = 1,2,\ldots,K(s)$, the PDF can be simply approximated as

$$p(k,s) \sim \hat{p}(k,s) = \frac{n(k,s)}{N-s+1}, \quad k = 1,2,\ldots,K(s), \quad (4)$$

The basic estimation of partition function reads,

$$\begin{aligned} z(s,q) &\equiv \sum_{k=1}^{K(s)} p^q(k,s) \\ \sim \hat{z}_n(s,q) &= \sum_{k=1}^{K(s)} \left[\frac{n(k,s)}{N-s+1}\right]^q \\ &\equiv \sum_{k=1}^{K(s)} \hat{z}_n(s,q,k). \end{aligned} \quad (5)$$

Assuming the time series behaves multifractal, we have the power laws [1],

$$\hat{z}_n(s,q) \sim s^{-\tau(q)}, \quad q \in (-\infty,+\infty). \quad (6)$$

A large value of q will enlarge significantly the differences of contributions from big and small probabilities and consequently extract the scaling behaviors obeyed by the component of big probabilities. On the other hand, a negative value of q will filter out the contributions of the large probabilities and expose the scaling behaviors in the component of small probabilities. The structure of the scaling behaviors, i.e., the density of components characterized by the scaling exponent $\tau(q)$, can be described by the multifractal spectrum, defined by the Legendre transform of $\tau(q)$ [100,101], which reads,

$$h = \frac{d\tau(q)}{dq}, \quad D(h) = qh - \tau(q), \quad (7)$$

where h is the local Hurst exponent and the relation of $D(h)$ versus h is the multifractal spectrum. One can measure the characteristics of the spectrum by the point at which $D(h)$ reaches the maxima, denoted with $[h_{\max}, D(h_{\max})]$, and the strength of multifractal defined as $\Delta h = h(q\to-\infty) - h(q\to+\infty)$. In the special case of h(q)=$\frac{d\tau(q)}{dq} = H =$ const, all the components obey the same power law. The multifractal degenerates to a monofractal.

In calculations, numerical derivative of $\tau(q)$ usually leads to unacceptable errors. Herein we employ the solution proposed by Kantelhardt [50], i.e., fitting the discrete points of $\tau(q)$ obtained from empirical records with an analytical expression, which reads,

$$\tau(q) = -\frac{\ln(x^q + y^q)}{\ln 2}. \quad (8)$$

The multifractal strength is $\Delta h = \frac{|\ln x - \ln y|}{\ln 2}$.

From the viewpoint of statistics, the simple approximation of PDF in Eq. (4) requires an infinite length of the initial time series ξ, namely, $N \to \infty$. In reality, however, the considered time series is generally very short, which may lead to unacceptable bias and statistical fluctuations to the estimated partition function $\hat{z}_n(s,q)$. Performance of an estimation should be measured by bias and standard deviation. As a simple illustration, we show herein the bias and variance of $\hat{z}_n(s,q)$ with a positive integer q.

For a specific system with its conditions keeping unchanged, it is reasonable to assume that the displacement's occurring probability distribution, $p(k,s), k = 1,2,\ldots,K(s)$, keep unchanged. If we conduct many times the measurements, from each measurement we can obtain a value of $n(k,s)$ corresponding to the kth bin, which is a realization of the probability $p(k,s)$. The measurements are independent of each other, namely, the deviation of $n(k,s)$ from the expected value of $Np(k,s)$ comes from uncorrelated noise. The realizations produced by this process obey a binomial distribution function (for simplicity $p(k,s)$ and $n(k,s)$ are denoted with p and n, respectively),

$$P(p,n,k,s) = \frac{(N-s+1)!}{n!(N-s+1-n)!} p^n (1-p)^{N-s+1-n}, \quad (9)$$

which will degenerate to Poisson and Gaussian distributions when N and p satisfy some special conditions. Hereafter, the statistical averages $\langle\cdot\rangle$ are all conducted over the binomial distribution.

A tedious computation (see Appendix for details) leads to the statistical average of the basic estimation of partition function,

$$\begin{aligned}\langle\hat{z}_n(s,q)\rangle &= \frac{1}{(N-s+1)^q}\sum_{k=1}^{K(s)}\langle n^q(k,s)\rangle \\ &= \frac{(N-s+1)!}{(N-s+1)^q}\sum_{k=1}^{K(s)}\sum_{j=0}^{q}\frac{S(q,j)}{(N-s+1-j)!}p^j(k,s) \\ &\equiv \sum_{k=1}^{K(s)}\langle\hat{z}_n(s,q,k)\rangle,\end{aligned} \tag{10}$$

where $S(q,j)$ is the Stirling numbers of the second kind, which can be generated iteratively as below [102],

$$S(i \geqslant 1,0) = 0, \quad S(i \geqslant 0, i \geqslant 0) = 1, \quad S(i+1,j) = S(i,j-1) + jS(i,j). \tag{11}$$

The bias from the kth term can be calculated with

$$\Delta\hat{z}_n(s,q,k) = \langle\hat{z}_n(s,q,k)\rangle - p^q(k,s), \quad k = 1,2,\dots,K(s). \tag{12}$$

For the special case of $q = 2$, we have the bias of the kth term,

$$\begin{aligned}\Delta\hat{z}_n(s,2,k) &= \frac{(N-s+1)p(k,s) + (N-s+1)(N-s)p^2(k,s)}{(N-s+1)^2} - p^2(k,s) \\ &= p^2(k,s)\left[\frac{1}{p(k,s)(N-s+1)} - \frac{1}{N-s+1}\right] \\ &\approx \frac{1}{\langle n(k,s)\rangle}p^2(k,s).\end{aligned} \tag{13}$$

Hence, when the average occurring number is small, the relative bias will reach unreasonably large. For instance, if $\langle n(k,s)\rangle = 5$ the relative bias is 20%.

By using a procedure analogous with that in Eq. (10), one can also estimate the statistical fluctuations for the terms in $\hat{z}_n(s,q)$, which read,

$$\begin{aligned}E_n(s,q,k) &\equiv \frac{1}{(N-s+1)^{2q}}\langle[n^q(k,s) - \langle n^q(k,s)\rangle]^2\rangle \\ &= \frac{1}{(N-s+1)^{2q}}\{\langle n^{2q}(k,s)\rangle - \langle n^q(k,s)\rangle^2\} \\ &= \frac{1}{(N-s+1)^{2q}}\left\{\sum_{j=0}^{2q}\frac{(N-s+1)!}{(N-s+1-j)!}S(2q,j)p^j(k,s) - \sum_{j_1,j_2=0}^{q}\frac{[(N-s+1)!]^2S(q,j_1)S(q,j_2)}{(N-s+1-j_1)!(N-s+1-j_2)!}p^{j_1+j_2}(k,s)\right\},\end{aligned} \tag{14}$$

where $k = 1,2,\dots K(s)$.

For the special case of $q = 2$, as an example, a simple computation leads to

$$\begin{aligned}E_n(s,2,k) &= \left[\frac{1}{(N-s+1)^3p^3(k,s)} + \frac{6(N-s)-1}{(N-s+1)^3p^2(k,s)} + \frac{4(N-s)(N-s-2)}{(N-s+1)^3p(k,s)} + \frac{2(N-s)(1-2N+2s)}{(N-s+1)^3}\right] \times p^4(k,s) \\ &\approx \left[\frac{1}{\langle n(k,s)\rangle^3} + \frac{6(N-s)-1}{(N-s+1)\langle n(k,s)\rangle^2} + \frac{4(N-s)(N-s-2)}{(N-s+1)^2\langle n(k,s)\rangle}\right] \times p^4(k,s),\end{aligned} \tag{15}$$

where for simplicity $N-s+1 \sim N$ is used. If N keeps unchanged, the value of $\langle n(k,s)\rangle$ will increases proportionally with $p(k,s)$. Hence, a large value of $p(k,s)$ means a large standard deviation of $\hat{z}_n(s,q)$.

B. Unbiased estimation of partition functions with positive integer q

Hence, the key problem is how to estimate the partition function $z(s,q)$ in Eq. (5) as precise as possible, i.e., to reduce the bias and statistical fluctuations simultaneously to minima. Let us consider first the case of q being a positive integer. Herein we will show that the goal can be realized by replacing the moment $n^q(k,s)$ with a q-order factorial moment [79–82], which reads,

$$F_q[n(k,s)] = n(k,s)[n(k,s)-1][n(k,s)-2]\dots[n(k,s)-q+1]. \tag{16}$$

The statistical average of the factorial moment reads ($p(k,s)$ and $n(k,s)$ are denoted with p and n respectively, for simplicity),

$$\begin{aligned}\langle F_q(n)\rangle &= \langle n(n-1)\dots(n-q+1)\rangle\\ &= \sum_{n=0}^{N-s+1}\frac{n!}{(n-q)!}\frac{(N-s+1)!}{n!(N-s+1-n)!}p^n(1-p)^{N-s+1-n}\\ &= \sum_{n=0}^{N-s+1}\frac{(N-s+1)!}{(n-q)!(N-s+1-n)!}p^n(1-p)^{N-s+1-n}.\end{aligned} \tag{17}$$

Because the terms with $n<q$ equal to zero, we can define $w=n-q$ and rewrite the average of $n(n-1)\dots(n-q+1)$ with

$$\langle F_q(n)\rangle = \sum_{w=0}^{N-s+1-q}\frac{(N-s+1)!}{w!(N-s+1-w-q)!}p^{w+q}(1-p)^{N-s+1-w-q} = \frac{(N-s+1)!}{(N-s+1-q)!}p^q. \tag{18}$$

Accordingly, by using the factorial moment we have an unbiased estimation of partition function, which reads,

$$\hat{z}_f(s,q) = \sum_{k=1}^{K(s)}\frac{(N-s+1-q)!}{(N-s+1)!}n(k,s)[n(k,s)-1]\dots[n(k,s)-q+1] \equiv \sum_{k=1}^{K(s)}\hat{z}_f(s,q,k). \tag{19}$$

Estimations of $\hat{z}_f(s,q)$ with different samplings will distribute randomly around the perfect value of partition function. As discussed in the remarks in subsection D, this kind of unbiased estimation of partition function values at different scales s can guarantee a minimum-variance mean-unbiased estimation of the slope of $\ln\hat{z}_f(s,q)$ versus $\ln s$ by using the ordinary least-square (OLS) regression method.

To evaluate the performance of this factorial-moment-based estimation, besides the statistical average's being unbiased we should also know its variance. Herein we derive the variances for the terms in $\hat{z}_f(s,q)$. Defining a set of integers $A=(a_1,a_2,\dots,a_Q)$, we have a simple fact that reads,

$$\prod_{j=1}^{Q}[n(k,s)+a_j] = \sum_{m=0}^{Q}C(m)n^{Q-m}(k,s), \tag{20}$$

where

$$C(0)=\frac{1}{0!}=1,\quad C(m)=\frac{\sum_{j_1\neq j_2\neq\dots\neq j_m=1}^{Q}a_{j_1}a_{j_2}\dots a_{j_m}}{m!},\quad m=1,2,3,\dots,Q, \tag{21}$$

based upon which one has the variance of the quantity defined in Eq. (20),

$$\begin{aligned}e_f(s,Q,k) &\equiv \left\langle\left\{\prod_{j=1}^{Q}[n(k,s)+a_j] - \left\langle\prod_{j=1}^{Q}[n(k,s)+a_j]\right\rangle\right\}^2\right\rangle\\ &= \sum_{m_1,m_2=0}^{Q}C(m_1)C(m_2)\langle n^{2Q-m_1-m_2}(k,s)\rangle - \sum_{m_1,m2=0}^{Q}C(m_1)C(m_2)\langle n^{Q-m_1}(k,s)\rangle\langle n^{Q-m_2}(k,s)\rangle\\ &= \sum_{m_1,m_2=0}^{Q}C(m_1)C(m_2)\left\{\sum_{j=0}^{2Q-m_1-m_2}\frac{(N-s+1)!S(2Q-m_1-m_2,j)}{(N-s+1-j)!}p^j(k,s)\right.\\ &\quad\left.-\sum_{j_1=0}^{Q-m_1}\sum_{j_2=0}^{Q-m_2}\frac{[(N-s+1)!]^2S(Q-m_1,j_1)S(Q-m_2,j_2)}{(N-s+1-j_1)!(N-s+1-j_2)!}p^{j_1+j_2}(k,s)\right\}\\ &= \frac{[(N-s+1)!]^2}{[(N-s+1-Q)!]^2}\sum_{m_1,m_2=0}^{Q}C(m_1)C(m_2)\left\{\sum_{j=0}^{2Q-m_1-m_2}\frac{[(N-s+1-Q)!]^2S(2Q-m_1-m_2,j)}{(N-s+1)!(N-s+1-j)!}p^j(k,s)\right.\\ &\quad\left.-\sum_{j_1=0}^{Q-m_1}\sum_{j_2=0}^{Q-m_2}\frac{[(N-s+1-Q)!]^2}{(N-s+1-j_1)!(N-s+1-j_2)!}S(Q-m_1,j_1)S(Q-m_2,j_2)p^{j_1+j_2}(k,s)\right\}\end{aligned}$$

$$\approx \frac{[(N-s+1)!]^2}{[(N-s+1-Q)!]^2} p^{2Q} \sum_{m_1,m_2=0}^{Q} C(m_1)C(m_2)$$
$$\left\{ \sum_{j=0}^{2Q-m_1-m_2} \frac{S(2Q-m_1-m_2,j)}{\langle n(k,s)\rangle^{2Q-j}} - \sum_{j_1=0}^{Q-m_1} \sum_{j_2=0}^{Q-m_2} \frac{S(Q-m_1,j_1)S(Q-m_2,j_2)}{\langle n(k,s)\rangle^{2Q-j_1-j_2}} \right\}. \tag{22}$$

The statistical fluctuation of the kth term in $\hat{z}_f(s,q)$ can be calculated as

$$E_f(s,q,k) = \left[\frac{(N-s+1-q)!}{(N-s+1)!}\right]^2 e_f(k,s)|_{(a_1,a_2,\ldots,a_Q)=(0,-1,-2,\ldots,-q+1)}, \tag{23}$$

where for simplicity $N \gg j, j_1, j_2, Q$ are used. If N keeps unchanged, the value of $\langle n(k,s)\rangle$ will increases proportionally with $p(k,s)$. Hence, a large value of $p(k,s)$ implies a large standard deviation of $\hat{z}_f(s,q)$.

C. Unbiased estimation of partition functions with noninteger q

In this part, based upon Eq. (19) we propose an unbiased estimation of partition functions with noninteger q. First, we employ the best square approximation [103] to mimic the term $p^q(k,s)$ in the partition functions, which is formulated as an optimization problem. The approximation expression reads,

$$\begin{aligned} &p^q \sim \sum_{i=0}^{I} b_i p^i, \\ &p = p(k,s), \quad k = 1,2,\ldots,K(s), \end{aligned} \tag{24}$$

where $b_i, i = 0,1,2,\ldots,I$ are expansion coefficients. To determine the expansion coefficients, we define the summation of the squares of residuals as

$$F(b_0,b_1,b_2,\ldots,b_I) = \int_{p_{\min}}^{1} \left(p^q - \sum_{i=0}^{I} b_i p^i\right)^2 dp, \tag{25}$$

where $p_{\min}$ is set to be sure the integrals in the following procedure are finite. The expansion coefficients are selected to make the function $F(b_0,b_1,b_2,\ldots,b_I)$ reach minima, which requires

$$\frac{\partial F(b_0,b_1,b_2,\ldots,b_I)}{\partial b_i} = 0, \quad i = 0,1,2,\ldots,I. \tag{26}$$

A simple computation leads to the values of the expansion coefficients,

$$b_i = \sum_{j=0}^{I} [C^{-1}]_{ij}[D]_j, \tag{27}$$

where the elements of the matrices C and D read,

$$\begin{aligned} C_{ij} &= \int_{p_{\min}}^{1} p^{i+j} dp = \frac{1-p_{\min}^{i+j+1}}{i+j+1}, \\ D_i &= \int_{p_{\min}}^{1} p^{q+i} dp = \frac{1-p_{\min}^{i+q+1}}{q+i+1}, \\ &i = 0,1,2,\ldots,I; j = 0,1,2,\ldots,I. \end{aligned} \tag{28}$$

In numerical calculations, the contribution of the terms with $n(k,s) = 0, k = 1,2,\ldots,K(s)$ are neglected. Consequently, a proper selection of $p_{\min}$ is $\frac{1}{N-s+1}$, though for $q > 0$ it can be assigned simply to be zero.

Second, inserting the approximation in Eq. (24) into the partition functions in Eq. (5), one has

$$z(s,q) = \sum_{k=1}^{K(s)} \sum_{i=0}^{I} b_i p^i(k,s) = \sum_{i=0}^{I} b_i \sum_{k=1}^{K(s)} p^i(k,s). \tag{29}$$

By using the unbiased estimation $\hat{z}_f(s,q)$ in Eq. (19), we obtain the unbiased estimation of partition functions with noninteger q,

$$\begin{aligned} \hat{Z}_f(s,q) &= \sum_{i=0}^{I} b_i \hat{z}_f(s,i) \\ &= \sum_{i=0}^{I} b_i \sum_{k=1}^{K(s)} \frac{n(k,s)}{N-s+1} \frac{n(k,s)-1}{N-s} \cdots \frac{n(k,s)-i+1}{N-s+2-i} \\ &= \sum_{k=1}^{K(s)} \left[\sum_{i=0}^{I} b_i \frac{n(k,s)}{N-s+1} \frac{n(k,s)-1}{N-s} \cdots \frac{n(k,s)-i+1}{N-s+2-i}\right] \\ &\equiv \sum_{k=1}^{K(s)} \hat{Z}_f(s,q,k). \end{aligned} \tag{30}$$

Obviously, when q is an integer, $\hat{Z}_f(s,q)$ degenerates to $\hat{z}_f(s,q)$ in Eq. (19).

As a brief summary, we propose in this work a procedure to evaluate multifractal behaviors embedded in a very short (stationary) time series, herein called FM-based evaluation of multifractals. The algorithm is realized with four steps.

Step 1: Map the time series to a stochastic process. Let a window with size s slide along the original stationary time series with length N. The covered segments form an ensemble of a stochastic process containing a total of $N - s + 1$ realizations (trajectories), as shown in Eq. (2);

Step 2: Find the distribution of the stochastic process. We calculate the summation of the elements in every segment, called displacement of the corresponding trajectory. Then one can find the distribution interval of all the displacements and divide it into a total of $K(s)$ bins. The width of a bin is selected to be a certain fraction (e.g., $\frac{1}{2}$) of the standard deviation of the initial time series. The distribution can be estimated by the number of displacements that occur in every bin, denoted with $n(k,s), k = 1,2,\ldots,K(s)$ [see Eqs. (3) and (4)];

Step 3: Calculate the FM-based estimation of partition function (an unbiased estimation). Let us specify first the values of q, e.g., $0.50, 0.55, 0.60, \ldots, 5.0$. For each value of q, given an approximation precision in Eq. (24) (e.g., 10^{-6}), one can determine the minimum expansion order, I, that makes the approximation errors for all the $p^q(k,s), k = 1,2,\ldots,K(s)$ are within the predefined precision, from which the values of expansion coefficients $b_0, b_1, \ldots, b_I$ can be determined further by using Eq. (27). The partition functions with different values of q can be estimated by using Eq. (30);

Step 4: Evaluation of multifractals. We select different values of window size s and for each specific value of s iterate Step 1 to Step 3. This procedure will generate curves of $\ln \hat{Z}_f(s,q)$ versus $\ln(s)$ with different values of q. If the curves obey power law, the multifractal spectrum can be calculated straightforwardly according to Eqs. (6) to (8).

D. Several remarks

The integer-q-order factorial moment is initially designed to discover dynamical behaviors embedded in records of high-energy collision experiments [79–82]. The standard scheme of the approach contains four steps. First, let us collect all the experiments and divide the phase space occupied by the produced particles into $L(s)$ bins with a window size of s each. For every experiment we count the number of particles occurring in each bin of the phase space, denoted with $n_r(k,s)$, where $r = 1,2,\ldots,R$ are a total of R experiments, and $k = 1,2,\ldots,K(s)$ the total of $K(s)$ bins. Second, by using $\hat{z}_f(s,q)$ in Eq. (19) we calculate the unbiased estimation of partition function for every experiment, denoted with $\hat{z}^r_f(s,q), r = 1,2,\ldots,R$. Third, the statistical average over all the experiments, i.e., $\langle \hat{z}_f(s,q)\rangle = \frac{1}{R} \times \sum_{r=1}^{R} \hat{z}^r_f(s,q)$, is used to approximate the partition function. Fourth, iteration of the above three steps with different window size s and the order q will generate curves of $\hat{z}_f(s,q)$ versus s for each specified q. If the curves obey power law, the dynamical process behaves intermittently (multifractal). A large amount of works on high-energy collision experiments show that $R = 20 \sim 30$ can guarantee high performance of the factorial moment approach [81,82].

An analogous procedure to detect multifractals in time series requires also an average procedure over a certain number of time series. However, this requirement cannot be fulfilled in most cases. For instances, the dynamical process of an earthquake produces only a single time series. An alternative way of statistical average is to separate a single time series into R parts as being a bundle of realizations. Obviously, it requires the time series being long enough, which is not the focus of the present work.

As described in the algorithm mentioned above, for a single short time series, we employ simply $\hat{Z}_f(s,q)$ in Eq. (30) to estimate the partition functions, i.e., no statistical average is conducted. Fortunately, we are interested in the scaling behavior, namely, the slope of $\ln \hat{Z}_f(s,q)$ versus $\ln(s)$. It is well-known that the ordinary least-square regression (OLS) method can provide a minimum-variance mean-unbiased estimation of the slope, if the errors for different points of s are homoscedastic and serially uncorrelated [104]. In this paper, we use the OLS method to estimate the scaling exponents, which guarantees a reliable result, even though we have only a single unbiased estimation of $\hat{Z}_f(s,q)$ at each specific point of s. The key factor leading to bias in the scaling exponent is the bias in estimations of partition function, which has been solved successfully by the FM-based estimation.

The confidence interval of the estimated scaling exponent is mainly determined by the errors of partition functions at different points of s, which can be roughly measured by the variance of $\hat{Z}_f(s,q)$. Here we assume that the terms, $\hat{Z}_f(s,q,k)$ with $k = 1,2,\ldots,K(s)$, are independent of each other, namely, a total of $K(s)$ independent stochastic variables. We denote their distribution functions and the corresponding standard deviations with $W[\hat{Z}_f(s,q,k)]$ and $\sigma(s,q,k), k = 1,2,\ldots,K(s)$, respectively. Obviously, the standard deviation of the mean of the stochastic variables will be

$$\sigma(s,q) = \frac{\sqrt{\sum_{k=1}^{K(s)} \sigma^2(s,q,k)}}{K(s)} = \frac{\langle \sigma(s,q,k)\rangle_k}{\sqrt{K(s)}}, \quad (31)$$

where $\langle\cdot\rangle_k$ is the statistical average over k. Hence, the summation in calculation of $\hat{Z}_f(s,q)$ will reduce the standard deviation of the estimated partition function by $\frac{1}{\sqrt{K(s)}}$.

As shown in Eq. (13), the bias in the basic estimation $\hat{z}_n(s,q)$ will be unreasonably large when the average $\langle n(k,s)\rangle$ is very small. While the standard deviations in the basic estimation $\hat{z}_n(s,q)$ and the FM-based estimation $\hat{Z}_f(s,q)$ will be significantly large when $p(k,s)$ is large. At the beginning the number of bins $K(s)$ is small and the occurring probabilities in the bins are large, and subsequently the statistical fluctuations are ignorable. While for s becoming large, the displacements will distribute in a wide range that implies the average occurring number in each bin is small. The number of bins $K(s)$ becomes subsequently large, which can reduce the standard deviation as shown above.

E. Standard tools for evaluating multifractals

The performance of the FM-based evaluation of multifractals is compared with the well-established tools in literature, including the wavelet transform modulus maxima (WTMM) and the multifractal detrended fluctuation analysis (MF-DFA).

Let us start from a nonstationary time series, $\theta = \{\theta_1,\theta_2,\ldots,\theta_N\}$. In the MF-DFA method [53,105–108], one constructs first from the initial time series a profile, whose ith element is the summation of the elements from θ_1 to θ_i, namely, $\Theta_i = \sum_{j=1}^{i}\theta_j, i = 1,2,\ldots,N$. Second, separating the profile into a total of $M(s) = \mathrm{int}[\frac{N}{s}]$ nonoverlapping segments with a predefined window size s and fitting every segment with a polynomial function, the resulting curves are regarded as trends for their corresponding segments. Here $\mathrm{int}[\cdot]$ is the roundoff number. Subtracting the trends from the profile results in a stationary series, $\Theta^s = \{\Theta_1^s,\Theta_2^s,\ldots,\Theta_{sM(s)}^s\}$. If the partition function behaves power law, i.e.,

$$\hat{Z}_{\mathrm{mfdfa}}(s,q) \equiv \frac{1}{M(s)s}\sum_{i=1}^{M(s)s}\left|\Theta_i^s\right|^q \sim s^{\kappa(q)}, \qquad (32)$$

the initial series behaves multifractals. In calculations, the order of the polynomial function is selected to be 2.

In the WTMM method [29,109–111], one should select a proper wavelet $\psi(\frac{i-b}{s})$ and let it slide along the series θ, namely, $b = 0,1,2,\ldots,N$. At every specific value of b, we calculate the wavelet transform coefficient, which reads

$$\eta_b(s) = \sum_{i=1}^{N}\psi\left(\frac{i-b}{s}\right)\theta_i. \qquad (33)$$

All the coefficients forms a series $\{\eta_1(s),\eta_2(s),\ldots,\eta_N(s)\}$. Finding all the coefficients at which the coefficient reaches local maxima, denoted with $\{\eta_1^{\max}(s),\eta_2^{\max}(s),\ldots,\eta_V^{\max}(s)\}$, where V is the total number of local maxima, the partition function is defined to be

$$\hat{Z}_{\mathrm{wtmm}}(s,q) \equiv \sum_{i=1}^{V}\left[\eta_i^{\max}(s)\right]^q. \qquad (34)$$

For a multifractal series, it satisfies a power law, $\hat{Z}_{\mathrm{wtmm}}(s,q) \sim s^{\chi(q)}$. In our calculations the wavelet is selected to be the second differential of Gaussian function, which can eliminate the trend in the series θ up to the second order.

As for the window size, because we are interested in scaling behaviors, the scale ranges, for instance, of 2^0–2^1, 2^1–2^2, 2^2–2^3, and 2^3–2^4 should have the same contributions in estimating the scaling exponents ($\tau(q)$, $\kappa(q)$, and $\chi(q)$). The window sizes are selected to be $s = [1.1^m], m = 1,2,\ldots$, where $[\cdot]$ is the integer part of a real number. If we plot the curve of logarithm value of partition function versus logarithm value of window size s, the points are distributed at almost identical intervals along the $\log(s)$ axis. Accordingly, in the least-square estimate of the scaling exponents, all the scales contain almost the same number of points and consequently have identical contributions.

III. MATERIALS

A. Probability redistribution model

The performance of our method is confirmed by multifractals generated with the probability redistribution (PRD) model. Let us define a vector as generator, which reads,

$$G_0^\beta = [\beta,1-\beta], \quad 0 \leqslant \beta \leqslant 1. \qquad (35)$$

At each generation, every element (probability) is redistributed into two new elements according to the generator, namely,

$$\begin{aligned} G_1^\beta &= [1]\otimes G_0^\beta = [\beta,1-\beta],\\ G_2^\beta &= G_1^\beta \otimes G_0^\beta = [\beta^2,(1-\beta)\beta,\beta(1-\beta),(1-\beta)^2],\\ &\ldots\\ G_g^\beta &= G_{g-1}^\beta \otimes G_0^\beta. \end{aligned} \qquad (36)$$

At the gth generation, the initial probability is separated into 2^g subelements. To cite an example, if the generator is selected to be [0.3,0.7], one has $G_2^{0.3} = [0.3,0.7]\otimes[0.3,0.7] = [0.3^2,0.7\times0.3,0.3\times0.7,0.7^2]$. The generated probability distribution G_g^β behaves exactly multifractal, whose elements are denoted with $G_g^\beta(k), k = 1,2,\ldots,2^g$.

We sample according to the uniform distribution N times and reckon the number of the samplings occurring in the intervals of

$$\begin{aligned} &\left[0,G_g^\beta(1)\right],\\ &\left(G_g^\beta(1),G_g^\beta(1)+G_g^\beta(2)\right],\\ &\ldots\\ &\left(\sum_{i=1}^{m}G_g^\beta(i),\sum_{i=1}^{m+1}G_g^\beta(m+1)\right],\\ &\ldots;\\ &\left(\sum_{i=1}^{2^g-1}G_g^\beta(i),\sum_{i=1}^{2^g}G_g^\beta(i)\right], \end{aligned} \qquad (37)$$

respectively, denoted with $\vec{n}_g = [n_1,n_2,\ldots,n_{2^g}]$. The vector $\vec{n}_g$ is a realization of the perfect multifractal G_g^β.

B. Gait time series

Two empirical records are investigated. The first case is to monitor the evolution of scaling invariance embedded in gait time series. The data is downloaded from the famous website www.physionet.org. The experiment recorded gaits for a total of ten young healthy volunteers [112,113], denoted with $si01,si02,\ldots,si10$, respectively. Here "health" implies that the participants have no history of any neuromuscular, respiratory, or cardiovascular disorders and are taking no medication. The ages are from 18 to 29 years. The height and weight center at 177 cm and 71.8 kg, with standard deviations of 8 cm and 10.7 kg, respectively. All the subjects walk continuously on level ground around an obstacle-free, long either 225- or 400-m, approximately oval path. The stride interval is measured by using an ultrathin, force-sensitive switch taped inside one shoe. Each subject walks for four trials, including slow, normal, fast, and metronome-regulated.

C. Shanghai stock market index series

The second case is to detect multifractal behaviors of the Shanghai stock market, embedded in the closing stock price series [114]. A series containing a total of 5350 closing stock prices is collected which covers a duration of 21 years from 1995 to 2015. The time series is separated into seven parts covering three years each, denoted with 95–97, 98–00, 01–03, 04–06, 07–09, 10–12, and 13–15, respectively. We will focus our attention on the comparison of multifractal behaviors between the different periods. To avoid trend effect on the calculated results, the daily return series is employed, which is defined herein as

$$r_k = \frac{\log_2 O_{k+1}}{\log_2 O_k}, \quad k = 1,2,\ldots,D-1, \tag{38}$$

where O_k is the closing stock price at the kth day, and D the total records in the considered series.

IV. RESULTS

A. Performance of FM-based evaluation of p^q

The key contribution of the present work is the explicit expression of $\hat{Z}_f(s,q,k)$ in Eq. (30), i.e., an unbiased estimation of $p^q(s,k)$. As a first step, we compare its performance with that of the basic estimation, $\hat{z}_n(s,q,k) \equiv [\frac{n(k,s)}{N-s+1}]^q$, as defined in Eq. (5). Specifying a probability p, let us generate a total of N random numbers uniformly distributed in the interval $[0,1]$, and reckon the number of the values occurring in the interval of $[0,p]$, herein called a realization. Obviously, the realization obeys a binomial distribution.

Figure 1 presents the biases and the standard deviations for the basic and the FM-based estimations of p^q with integer q. Here the curves for $q = 2$, $N = 300$ are shown as a typical result. The statistical averages are conducted over 50 000 realizations. One can find from Fig. 1(a) that the calculated bias for the basic estimation increases with probability, while that for the FM-based estimation oscillates with small amplitudes around the *probability* axis (zero). The calculated bias are all consistent with the theoretical

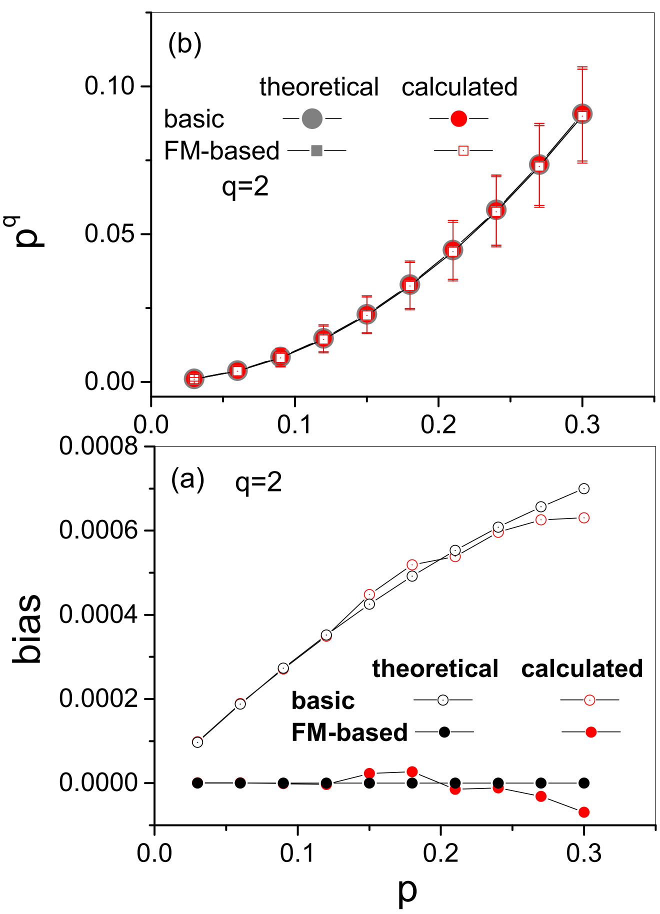

FIG. 1. Bias and fluctuation in estimation of p^q with positive integer q. For every specified probability a total of 300 samplings are used to generate a realization. Each bias and each standard deviation are calculated over 50 000 realizations. Curves with $q = 2$ are shown as typical results. (a) Biases for the basic and the FM-based estimations. The basic estimation leads to significant bias, while the bias is eliminated in the FM-based estimation. (b) Standard deviations for the basic and FM-based estimations.

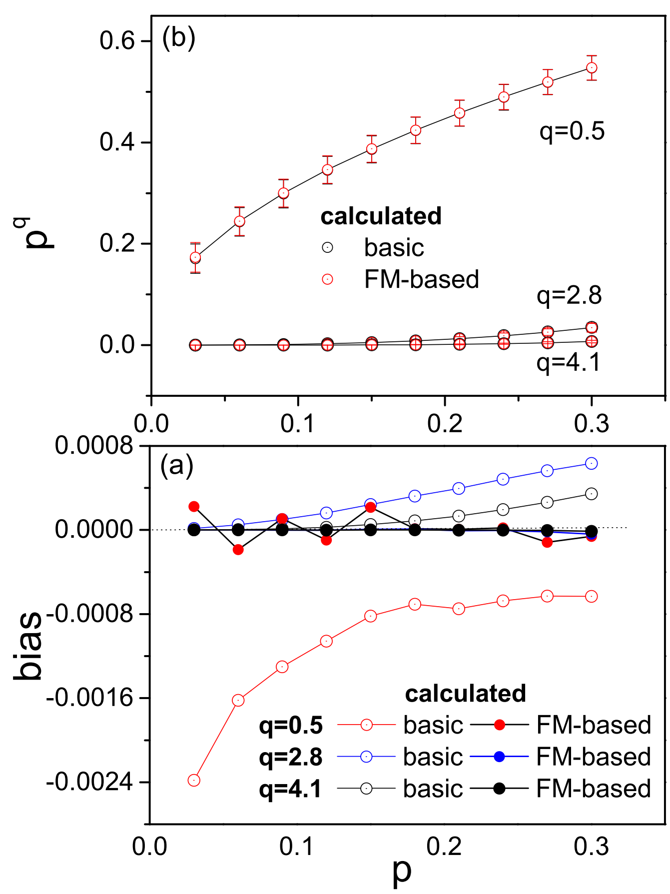

FIG. 2. Bias and fluctuation in estimation of p^q with positive noninteger q. Curves for $q = 0.5, 2.8$, and 4.1 are shown as typical examples. For each specified probability a total of 300 samplings are used to generate a realization. Each bias and each standard deviation are calculated over 50 000 realizations. (a) Biases for the basic and the FM-based estimations. The basic estimation leads to significant bias, while the bias is eliminated in the FM-based estimation; (b) standard deviations for the basic and the FM-based estimations.

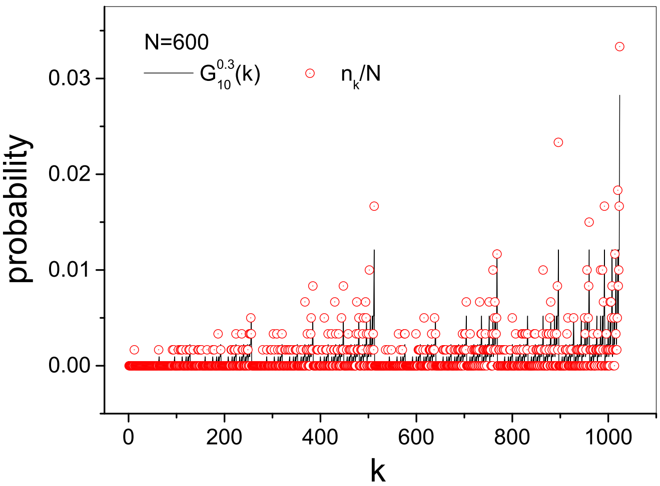

FIG. 3. A typical example of multifractal generated with the probability redistribution (PRD) model. Black curve: probability distribution of $G_{10}^{0.3}$ produced with $G_0^\beta = [0.3,0.7]$ and $g = 10$. Red open circle: a realization with $N = 600$ samplings.

predictions. The standard deviations for the two estimations are almost the same and increase monotonically with probability [see Fig. 1(b)]. Analogous results with noninteger q are shown in Fig. 2 ($q = 0.5, 2.8$, and 4.1).

B. Performance of FM-based evaluation of multifractals

By using the PRD model one can generate a perfect multifractal G_g^β. Figure 3 shows the structure of $G_{10}^{0.3}$. A realization with $N = 600$ is also provided with the open red circles.

Figure 4 depicts estimations of partition functions for multifractals generated with the generators $G_0^\beta = [0.3, 0.7]$ and $G_0^\beta = [0.4, 0.6]$, the total number of samplings $N = 300, 600$, and the number of generations $g = 10$. To make the illustration be consistent with that for multifractals in time series, we convert the generation to a window size, defined as being the reciprocal of the total number of probabilities in the generation, denoted with win. For instance, in the 4th generation there are 2^4 probabilities, the corresponding window size is $win = \frac{1}{2^4}$. With the increase of generation, namely, the initial probability is redistributed into many probabilities, the basic estimation will deviate significantly from the exact value. The deviation will become much larger when β in $G_0^\beta = [\beta, 1-\beta]$ becomes closer to 0.5, namely, the probability distribution is comparatively homogenous. While the FM-based estimation keeps very close to the exact value. The averages and deviations are calculated over 1000 realizations.

From the partition functions for four single realizations ($N = 300, 600$, $G_0^\beta = [0.3,0.7], [0.4,0.6]$, and $g = 10$), one can obtain the relations of τ_q versus q, and the multifractal spectra (see columns (a), (b), and (c) in Fig. 5, respectively). The FM-based estimations of τ_q versus q and $D(h)$ versus h are very close to or even coincident exactly with the theoretical curves. On the contrary, the basic estimations will lead to significant errors, or even mistakes. Here we fit the partition

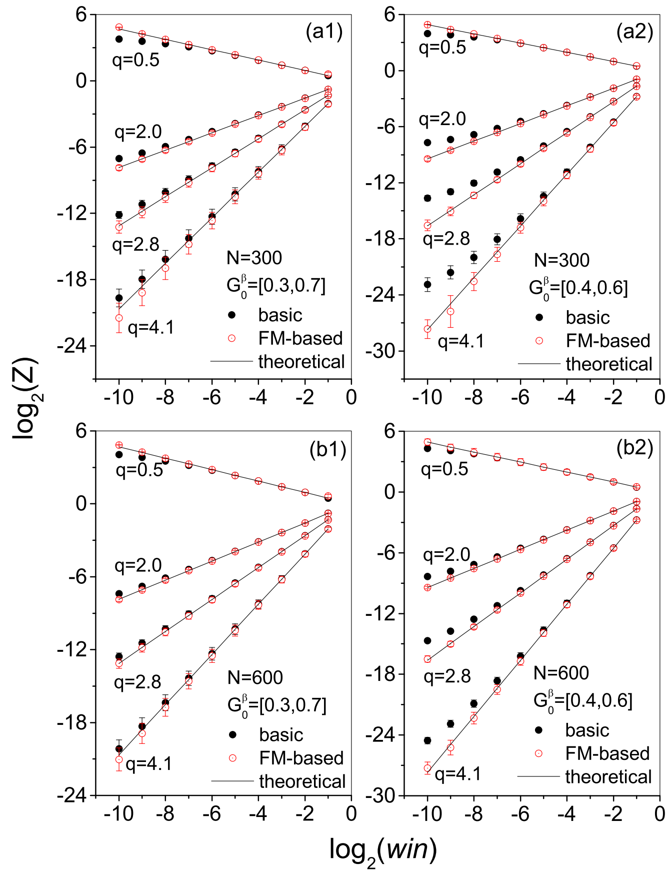

FIG. 4. Four typical estimations of partition functions for multifractals generated with the probability redistribution (PRD) model. Corresponding to the gth generation, we define the window size win as being the reciprocal of the total number of probabilities contained in G_g^β, namely, $\frac{1}{2^g}$. Statistics are conducted over 1000 realizations. (a1) $G_0^\beta = [0.3,0.7]$, $N = 300$, $g = 10$. (a2) $G_0^\beta = [0.4,0.6]$, $N = 300$, $g = 10$. (b1) $G_0^\beta = [0.3,0.7]$, $N = 600$, $g = 10$. (b2) $G_0^\beta = [0.4,0.6]$, $N = 600$, $g = 10$. With the increase of generation, the basic estimation will deviate significantly from the exact value. The deviations for $G_0^\beta = [0.4,0.6]$ are larger than the corresponding values for $G_0^\beta = [0.3,0.7]$. While the FM-based estimation keeps very close to the exact value.

functions with the power-law function no matter if there exists significant biases or not. The curve of τ_q versus q obtained with the basic estimation will bend down in a comparatively significant way with the increase of q. Consequently, the basic estimation will give unreasonably wider distribution of fractal dimension (Δh) at the left side of the spectrum, that corresponds to the components extracted with larger values of q.

C. Evolution of multifractals in gait time series

As a typical example, we consider here the fast, normal, and slow trials for the volunteer numbered $si09$. The metronome-regulated trial is not shown, because it behaves simply random (Hurst exponent is 0.5). From each gait series we extract five segments, which cover the elements 1–500, 501–1000, 1001–1500, 1501–2000, and 2001–2500, denoted

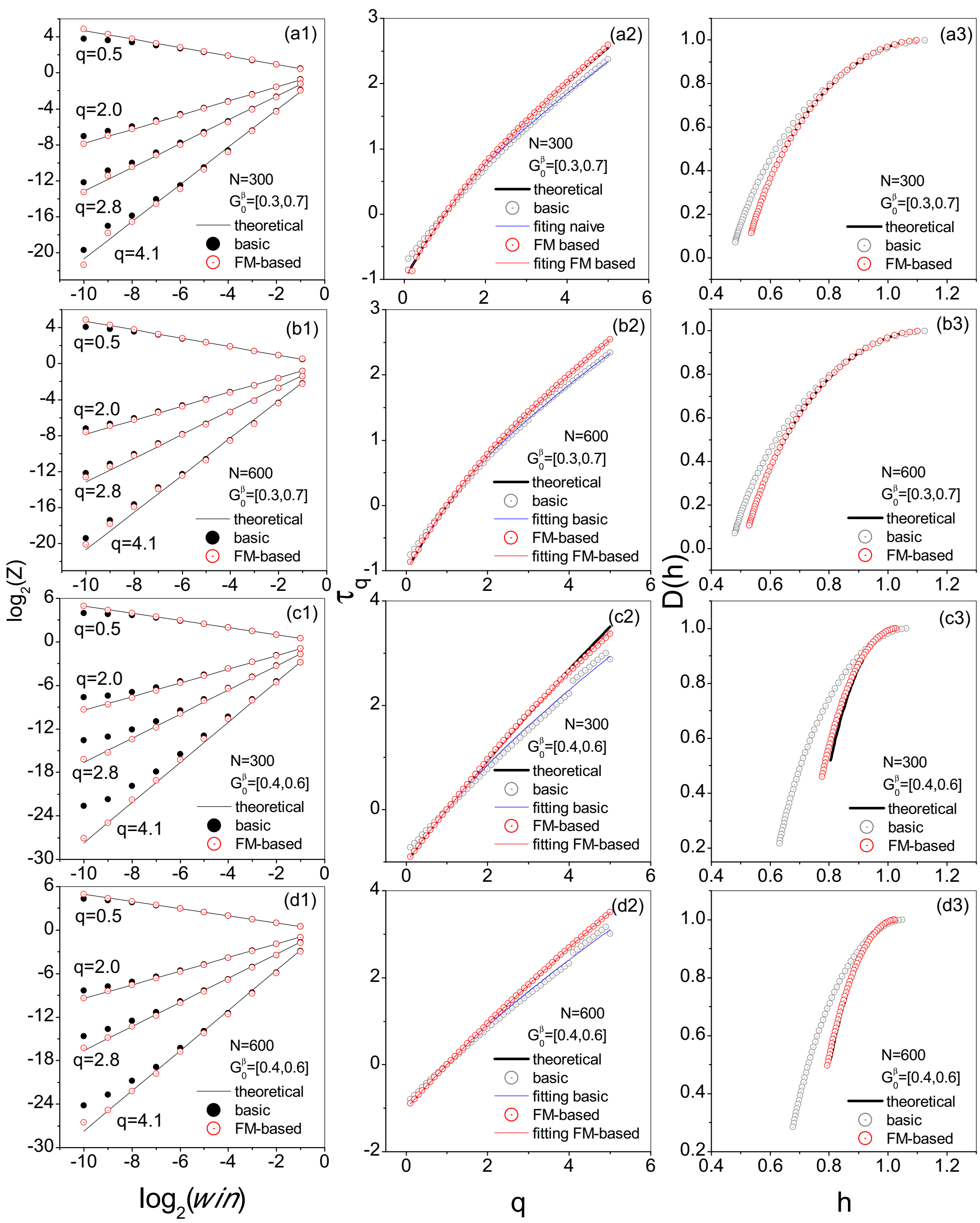

FIG. 5. Evaluation of multifractal spectrum from a single realization of the probability redistribution (PRD) model. Partition functions with $q = 0.5, 2.0, 2.8$, and 4.1 are shown as typical examples. The relations of partition function versus window size, τ_q versus q, and multifractal spectrum [$D(h)$ versus h] for four single realizations are displayed in rows (a), (b), (c), and (d), respectively. (a1–a3) $N = 300$, $G_0^\beta = [0.3, 0.7], g = 10$; (b1–b3) $N = 600$, $G_0^\beta = [0.3, 0.7]$, $g = 10$; (c1–c3) $N = 300$, $G_0^\beta = [0.4, 0.6]$, $g = 10$; (d1–d3) $N = 600$, $G_0^\beta = [0.4, 0.6]$, $g = 10$. The window size is defined to be the reciprocal of the number of probabilities in the generated probability distribution G_g^β, namely, $win = \frac{1}{2^g}$.

with *seg*-1,*seg*-2,*sge*-3,*seg*-4, and *seg*-5, respectively (see Fig. 6 for details).

Figures 7(a1)–(a5), 7(b1)–(b5), and 7(c1)–(c5) provide the partition functions for the fast, normal, and slow series. The shapes of partition function with different values of q are qualitatively similar. A larger value of q will simply enlarge the differences between the values in a curve. Hence we show only the curves for $q = 0.5$ and 2.3 as being representatives (the red circles). One can find that the partition functions obey power law in considerable wide scales (from 2^0 to $2^{5.7} \sim \frac{N}{10}$ or even to $2^{6.8} \sim \frac{N}{5}$).

As for the relations between τ_q and q (see Fig. 7(d1)–(d3), one can find that only the points for $q > 1$ can be fitted with the Eq. (8) very well, while that for $q < 1$ are significantly larger than the calculated points with the fitting function (the points are above the calculated values). How to understand the part for $q < 1$ is still an open problem to be fixed with much more data and detailed analysis.

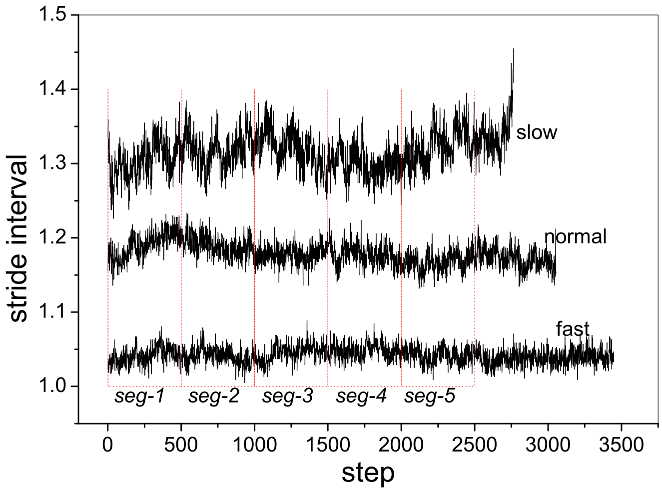

FIG. 6. Gait time series for the volunteer numbered *si*09. The fast, normal, and slow trials are shown. From each trivial we extract five successive segments covering the records 1–500, 501–1000, 1001–1500, 1501–2000, and 2001–2500, denoted with *seg*-1,*seg*-2,*seg*-3,*seg*-4, and *seg*-5, respectively.

The multifractal spectra for the fast, normal, and slow series (containing five segments each) are displayed in Figs. 7(e1)–(e3), from which one can find that the multifractal strength for the fast segments changes significantly, while that for the normal and slow trials have similar behaviors. The strengths for the three series distribute in [0.04,0.47], [0.16,0.27], and [0.13,0.29], respectively.

D. Multifractals in stock index series

The collected stock index series from the year 1995 to the year 2015 is separated into seven successive durations covering three years each, denoted with 95–97, 98–00, 01–03, 04–06, 07–09, 10–12, and 13–15, respectively (see Fig. 8 for details on the original series and the return series). In the two durations 95–97 and 07–09 occurred the famous Asia financial crisis in the year 1997 and the global financial crisis in the year 2008.

Figures 9(a1)–(a7) provide the partition functions with $q = 0.5$ and 2.8 as typical examples. One can find that the partition functions versus window size obey power-law with different slopes in considerable wide scales (red circles). Interestingly, in the two durations when crises occurred, i.e., 95–97 and 07–09 the partition function versus window size obey comparatively much perfect power law and in much larger scales (up to $2^{7.8} \sim 222$, a length covering about one year, i.e., one-third of the whole series length), as presented in Figs. 9(a2) and 9(a5).

As for the relations between τ_q and q (see Figs. 9(b1)–(b4), one can find that they behave similar with that of the gait time series. The points for $q > 1$ can be fitted with the Eq. (8) very well, while that for $q < 1$ are significantly larger than the calculated points with the fitting function. Much more data and detailed analysis are required to fix this open problem.

The multifractal spectra for the seven durations are displayed in Fig. 8(c), from which one can find that all the series have large multifractal strengths, values of which are 0.99, 0.68, 0.99, 0.70, 0.63, 1.35, and 1.0 for the successive durations from 95–97 to 13–15, respectively. In the crisis duration 07–09 the multifractal strength becomes the weakest, namely, the local hurst exponents corresponding to q distribute in the sharpest range, while that for the following duration 10–12 has the widest distribution, which is regarded here as the intermediate state. The behaviors for the duration 04–06 (before crisis) and the duration 98–00 (after crisis) are very similar with that for the extreme case in the duration 07–09, all of which form a crisis-cluster. The behaviors for the other durations far from crises (95–97, 01–03, 13–15) are very similar and they form a distinguished normal cluster.

E. Comparison with the well-established tools

In Figs. 7 and 9, for every series segment we calculate also the partition functions with three well-established tools, including the WTMM, the MF-DFA, and the basic estimation. The FM-based estimation can capture the scaling behaviors of the partition functions in a considerable wide range from 2^0 to $2^{5.7} \sim \frac{N}{10}$ or even to $2^{6.8} \sim \frac{N}{5}$ for the gait time series ($N = 500$), and from 2^0 to $2^{6.7} \sim \frac{N}{5}$ or even to $2^{7.8} \sim \frac{N}{3}$ for the closing price series of the Shanghai stock market ($N \sim 670$), as mentioned above. The scale covers about 6 or even 8 generations. And the estimated values of partition function for every segment scattered closely around a power-law line. Here a generation is defined to be the doubling of the window size.

The MF-DFA-based estimations can detect the scaling behaviors only when the window size is larger than 2^3, i.e., the third generation. On the contrary, the basic estimation fails at the larger window sizes, where the curves bend down and can not detect qualitatively the scaling invariance.

To reach a reliable conclusion on existence of a scaling invariance, the key criterion is to find a reasonably wide range of scale in which the partition functions behave power law. The scale ranges, for instance, of 2^0–2^1, 2^1–2^2, and 2^3-2^4 are equivalent in the criterion. Hence, the generations covered by the scale range is much more important than the maximum scale the range reaches. Comparing with the MF-DFA and the basic estimation, the FM-based estimation can detect scaling invariance in a wide range of scale about three generations larger. It is a significant improvement of performance for very short time series.

As for the WTMM-based estimations, for all the segments they have unacceptable large fluctuations over all the generations of scale.

This advantage of FM-based estimation over the other standard tools is verified further by fractional Brownian motions (fBm). Figures 10(a1) and 10(a2) show the partition functions with $q = 0.6, 2.8$ and Hurst exponent $H = 0.65, 0.75$ as typical examples (length is selected to be 500). Similar evidences are found, namely, the FM-based estimation obey almost a perfect power law in a wide scale covering more than four generations, while the MF-DFA method can capture the scaling behaviors only in the scales larger than 2^3 that cover about two generations. The values of partition function

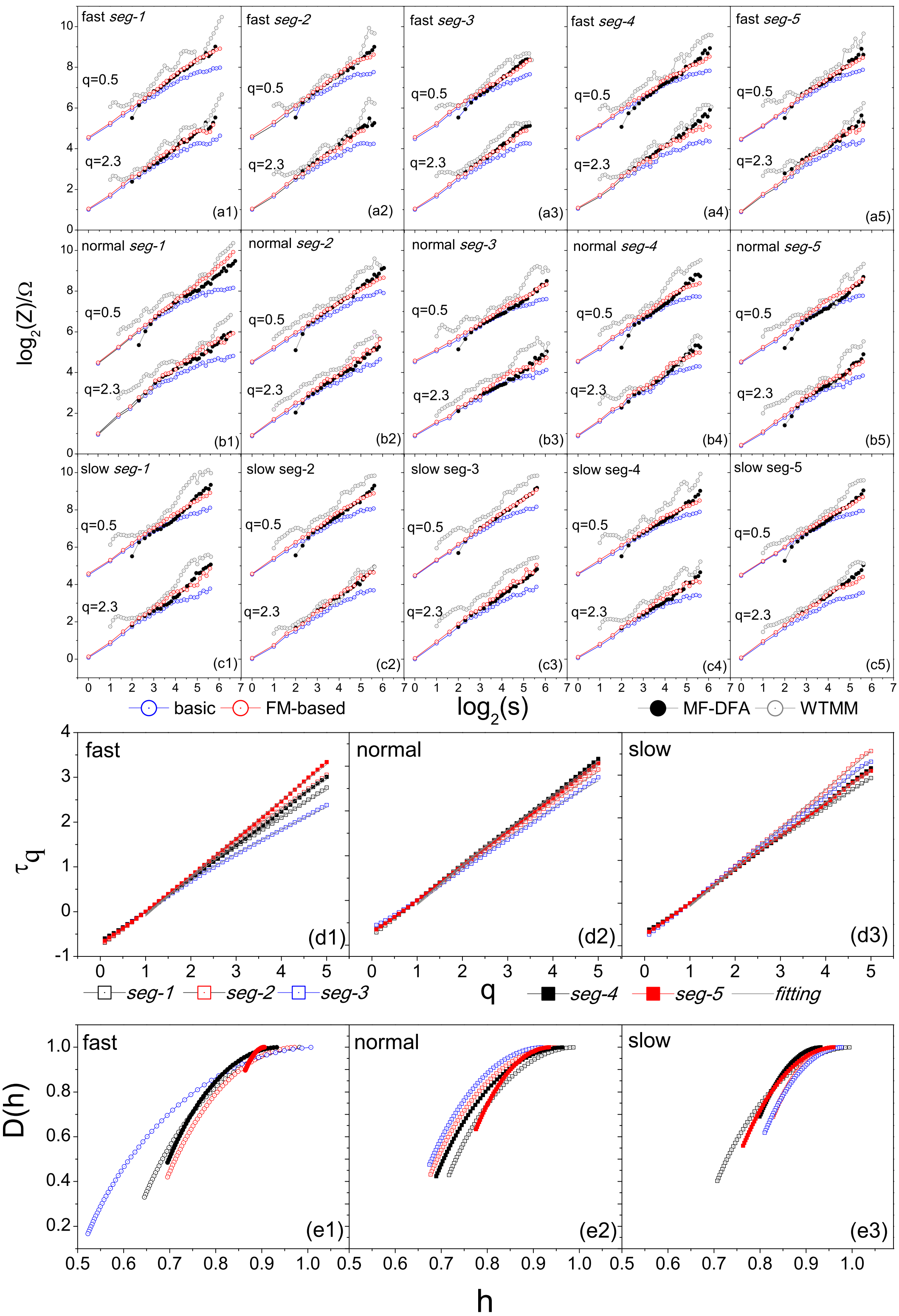

FIG. 7. Evolution of multifractals in gait series for the volunteer numbered *si*09. (a1–a5), (b1–b5), and (c1–c5) The partition functions for the fast, normal, and slow series, respectively. The curves with $q = 0.5$ and 2.3 are provided as representatives. The basic, FM-based, WTMM, and MF-DFA estimations are shown with the blue open circles, red open circles, gray open circles, and black solid circles, respectively. For visual convenience, the logarithm of partition function is rescaled with Ω. For the basic and FM-based method $\Omega = q - 1$, while for the WTMM and MF-DFA, $\Omega = q$; (d1–d3) The relations of τ_q versus q; (e1–e5) The multifractal spectra for the fast, normal, and slow series (containing five segments each).

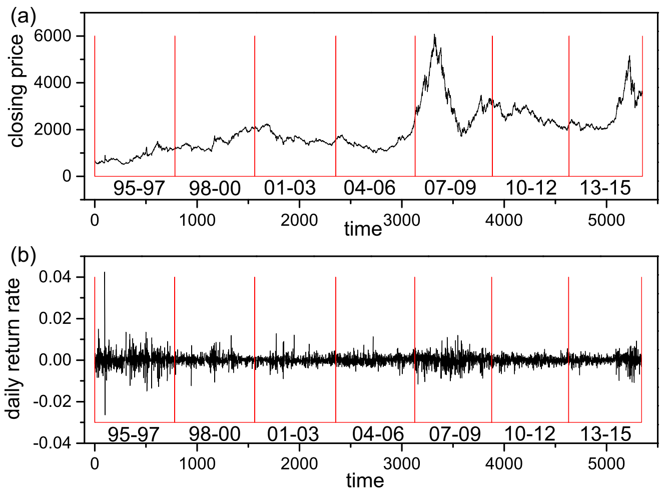

FIG. 8. Closing price series and return series for the Shanghai stock market. (a) The closing price series; (b) The corresponding return series. The time series covers a 21-year duration from 1995 to 2015, which is partitioned into seven segments covering three years each, denoted with 95–97, 98–00, 01–03, 04–06, 07–09, 10–12, 13–15, respectively.

estimated with WTMM scattered around a power-law curve with unacceptable large fluctuations.

Figures 10(b1), 10(b2), 10(c1), and 10(c2) provide the distributions of the estimated scaling exponents τ_q (rescaled for visual convenience). For each specified value of H we generate a total of 1000 fBm series and calculate the partition functions, from which one can evaluate the scaling exponents. Because the generated series are mono-fractals, the estimated values should distribute with the specified values of H as being the centers, respectively. The red curves (FM-based estimation) are the results fitting in the scale ranges of 2^0–$2^{3.5}$ (open circles) and 2^0–$2^{4.5}$ (solid circles), which turn out to be very close and their averages are very close with the expected values (H). The black curves (MF-DFA-based estimation) are the results fitting in the scale ranges of 2^2–2^5 (open circles) and 2^3–2^5 (solid circles). The part in the scale range of 2^2–2^3 leads to a unreasonably large estimations of scaling exponents. Hence, FM-based estimation can capture the scaling behaviors in much wider a scale range.

V. CONCLUSION AND DISCUSSION

In summary, multifractal exists in a large amount of series and has been making great contributions in diverse research fields. Some powerful methods such as the WTMM and the MF-DFA have been developed in literature. The tools require generally an infinite length (at least large enough a length) of time series. In reality, we have a finite number of records, which may lead to unacceptable errors or even mistakes to estimation of multifractals. How to evaluate exactly multifractal spectrum from a short time series is still an open problem.

In this paper, by means of approximation theory we propose a new method called continuous order FM-based estimation of multifractal. It is theoretically predicted and computationally confirmed that it can provide an unbiased estimation of partition functions, while its standard deviation is almost the same with that for the basic estimations. It can give almost exactly scaling behaviors embedded in very short time series with several hundred length.

Comparing with the well-established tools one can find that the continuous order FM can evaluate correctly the scaling behaviors in a wide scale (starting from 2^0) about three generations larger than that of the MF-DFA, in which the scale starts from 2^3. The basic estimation method fails in detecting the scaling behaviors at large scales (the partition function bends down). As for the WTMM, the estimated partition function has unacceptable fluctuations in the whole scale. It is a significant improvement of performance in detecting multifractals in very short time series.

Two empirical cases are investigated as typical examples. The first case is the gait time series for fast, normal, and slow trials of a healthy volunteer. The series are separated into five successive nonoverlapping segments with a 500 length each. It is found that the multifractal strength for the fast trial changes abruptly, while that for the normal and slow trials have similar behaviors. The second case is the closing price series for Shanghai stock market. The series is partitioned into seven successive periods covering three years each. Interestingly, the period from 2007 to 2009, which covers the famous global financial crisis occurring in 2008 is an extreme case with the weakest multifractal strength. The periods after the Asian financial crisis (from 1998 to 2000) and before the global financial cris (from 2004 to 2006) behave very similar with the extreme case, all of which form a crisis-cluster. After the extreme case follows a relaxation state with the strongest multifractal strength (from 2010 to 2012). While the other periods far from the crises, have also almost the same behaviors, which form a normal state cluster.

The key contribution in our work is that we develop a method to estimate without bias the probability moments of continuous order. It can be used to evaluate multifractals embedded in short time series with a several hundreds length as being the focus of the present work. However, one can find its applications in various problems beyond the measurement of scaling invariance. Actually, estimation of probability moments is the base of several essential theories. To cite examples, the continuous order FM can be used straightforwardly to estimate the Tsallis entropy to show nonextensive behavior of a complex system; to estimate mutual entropy and transfer entropy between elements in a complex system to find causality relationships between each pair of elements. When we analyze multivariate time series, finite number of records will lead to unreasonable bias and fluctuations because the finite recordings will distribute into bins whose number increases geometrically with variate number. Hence, to conduct empirically multivariate time series analysis, we should replace the basic estimation of probability moments with the FM-based estimation.

It should be noted that the proposed factorial moment of continuous order turns out to be valid only for positive order. How to extend it to negative order is still an open problem to be solved in future.

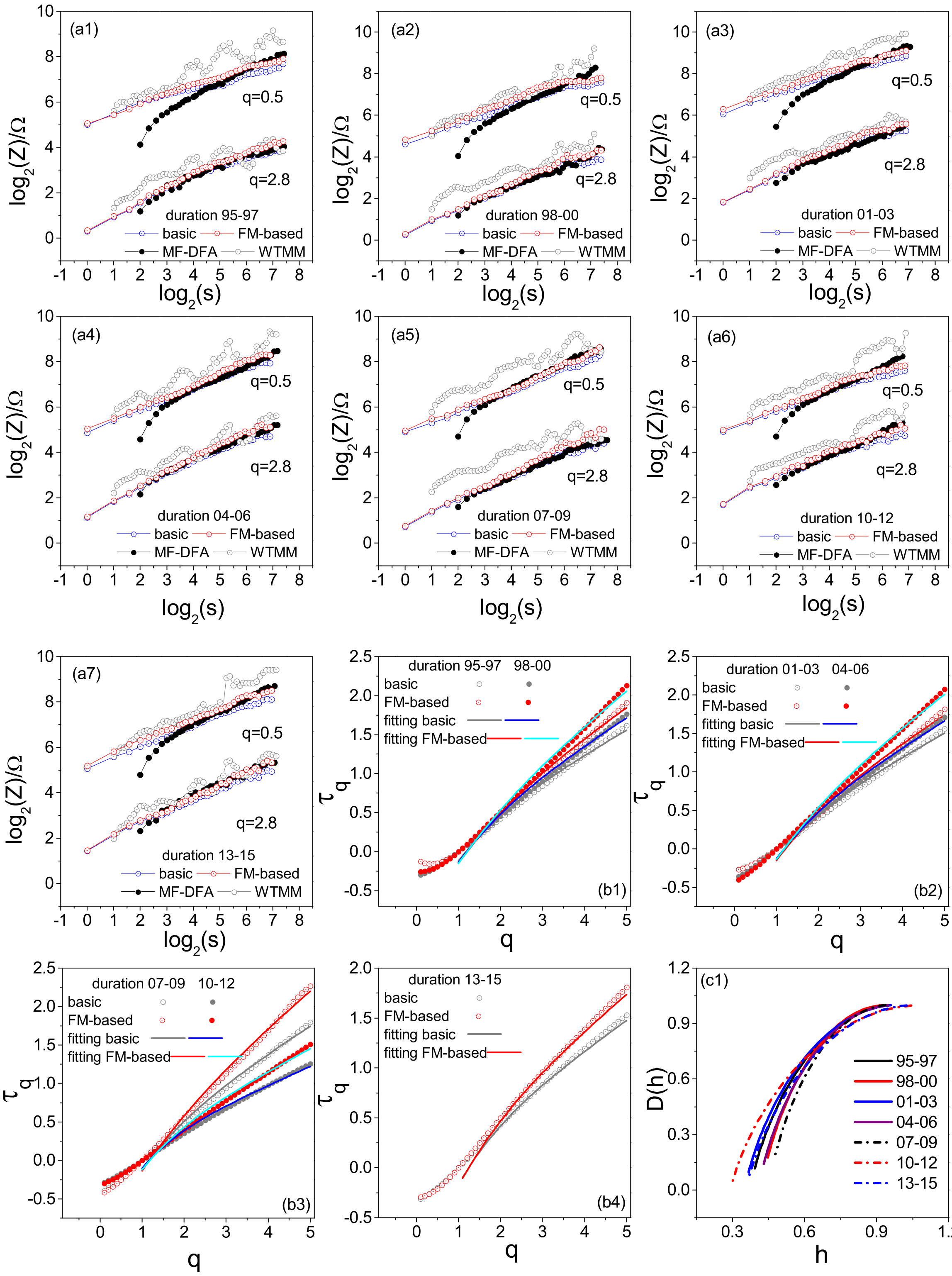

FIG. 9. Evolution of multifractals in Shanghai stock market index series. (a1–a7) The partition functions for the segments numbered 95–97, 98–00, 01–03, 04–06, 07–09, 10–12, and 13–15, respectively. Curves with $q = 0.5, 2, 2.8, 4.1$ are shown as typical examples. The basic, FM-based, WTMM, and MF-DFA estimations are shown with the blue open circles, red open circles, gray open circles, and black solid circles, respectively. For visual convenience, the logarithm of partition function is rescaled with Ω. For the basic and FM-based method $\Omega = q - 1$, while for the WTMM and MF-DFA, $\Omega = q$; (b1–b4) The relations between τ_q and q; (d1) The multifractal spectra for the seven durations.

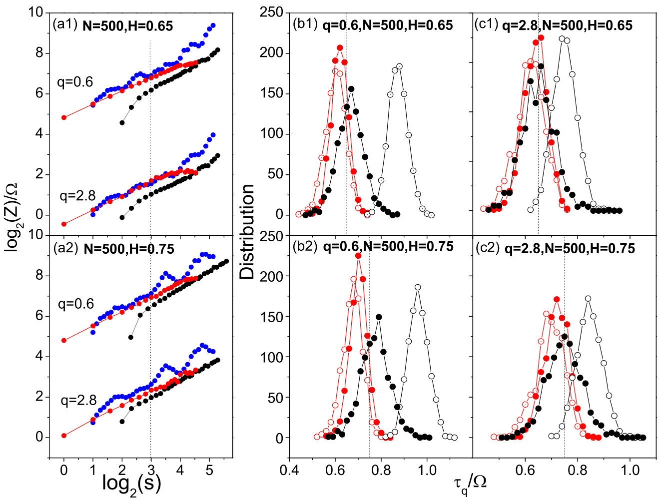

FIG. 10. Comparison of performance by using fractional Brownian motions. For each specified value of H we generate a total of 1000 fBm series and calculate the partition functions, from which one can evaluate the scaling exponents. Series length is selected to be 500. The red curves (FM-based estimation) are the results fitting in the scale ranges of 2^0–$2^{3.5}$ (open circles) and 2^0–$2^{4.5}$ (solid circles). The black curves (MF-DFA-based estimation) are the results fitting in the scale ranges of 2^2–2^5 (open circles) and 2^3–2^5 (solid circles). (a1–a2) The partition functions with $q = 0.6, 2.8$ and Hurst exponent $H = 0.65, 0.75$ as typical examples. The distributions of the estimated scaling exponents τ_q (rescaled for visual convenience) are shown in (b1) $H = 0.65, q = 0.6$; (b2) $H = 0.65, q = 2.8$; (c1) $H = 0.75, q = 0.6$; and (c2) $H = 0.75, q = 2.8$.

ACKNOWLEDGMENTS

This work is supported by the National Natural Science Foundation of China under the Grant No. 10975099 to Prof. Huijie Yang and the Grant No. 11505114 to Prof. Changgui Gu; the Shanghai Municipal Education Commission under the Grant No. 13YZ072 to Prof. Huijie Yang, the No. D-USST02 to Prof. Huijie Yang, and the Grant No. QD2015016 to Prof. Changgui Gu. It is also supported by the Shanghai Municipal Education Commission under Grant No. USST-02-SAI for disciplinary development of systematic analysis and integration. We thank the reviewers for their stimulating and constructive comments and suggestions.

APPENDIX

Before the derivation of the high-order moments, let us introduce several definitions and theorems.

Binomial distribution function. Let us sample a total of N times from the homogenous distribution in the interval of $[0,1]$ and reckon the number of the samplings occurring in the interval $[0,p]$ $(0 < p < 1)$. The distribution of n obeys the binomial distribution function, which reads,

$$P(n,p) = \frac{N!}{n!(N-n)!} p^n (1-p)^{N-n}. \tag{A1}$$

The q-order moment reads,

$$\langle n^q \rangle \equiv \sum_{n=0}^{N} n^q P(n,p) = \sum_{n=0}^{N} \frac{N! n^q}{n!(N-n)!} p^n (1-p)^{N-n}. \tag{A2}$$

The Stirling numbers of the second kind. The Stirling numbers of the second kind can be generated iteratively by using the relation

$$S(m,l) = l S(m-1,l) + S(m-1,l-1), \tag{A3}$$

accompanying with the initial values, $S(m \geqslant 1,0) = 0$, $S(0,0) = 1$, and $S(m \geqslant 0, m \geqslant 0) = 1$.

By using the Stirling numbers of the second kind, the term n^q in Eq. (A2) can be expressed with an expansion [102], which reads,

$$\begin{aligned} n^q &= S(q,0)[n]_0 + S(q,1)[n]_1 + \cdots + S(q,q)[n]_q \\ &= \sum_{l=0}^{q} S(q,l)[n]_l, \end{aligned} \tag{A4}$$

where $[n]_l \equiv \frac{n!}{(n-l)!}$.

Accordingly, one can derive the q-order moment [115]. Herein we consider only the case of q being a positive integer value:

$$\begin{aligned} \langle n^q \rangle &= \sum_{n=0}^{N} n^q \frac{N!}{n!(N-n)!} p^n (1-p)^{N-n} \\ &= \sum_{n=0}^{N} \sum_{l=0}^{q} S(q,l)[n]_l \frac{N!}{n!(N-n)!} p^n (1-p)^{N-n} \\ &= \sum_{l=0}^{q} \sum_{n=0}^{N} S(q,l) l! \frac{n!}{l!(n-l)!} \frac{N!}{n!(N-n)!} p^n (1-p)^{N-n} \\ &= \sum_{l=0}^{q} \sum_{n=l}^{N} S(q,l) l! \frac{n!}{l!(n-l)!} \frac{N!}{n!(N-n)!} p^n (1-p)^{N-n} \\ &= \sum_{l=0}^{q} S(q,l) l! \sum_{n=l}^{N} \frac{n!}{l!(n-l)!} \frac{N!}{n!(N-n)!} p^n (1-p)^{N-n} \\ &= \sum_{l=0}^{q} S(q,l) l! \sum_{r=0}^{N-l} \frac{(r+l)!}{l! r!} \frac{N! p^{r+l} (1-p)^{N-r-l}}{(r+l)!(N-r-l)!} \\ &= \sum_{l=0}^{q} S(q,l) l! p^l \sum_{r=0}^{N-l} \frac{(r+l)!}{l! r!} \frac{N! p^r (1-p)^{N-r-l}}{(r+l)!(N-r-l)!} \\ &= \sum_{l=0}^{q} S(q,l) \frac{N!}{(N-l)!} p^l \sum_{r=0}^{N-l} \frac{(N-l)!}{r!(N-r-l)!} p^r (1-p)^{N-r-l} \\ &= \sum_{l=0}^{q} S(q,l) \frac{N!}{(N-l)!} p^l \\ &= \sum_{l=0}^{q} S(q,l) [N]_l p^l. \end{aligned} \tag{A5}$$

[1] M. F. Barnsley, *Fractal Everywhere* (Academic Press, Orlando, 1993).
[2] N. Scafetta, P. Hamilton, and P. Grigolini, Fractals **9**, 193 (2001).
[3] P. Grigolini, L. Palatella, and G. Raffaelli, Fractals **9**, 439 (2001).
[4] N. Scafetta and P. Grigolini, Phys. Rev. E **66**, 036130 (2002).
[5] J.-J. Huang, P.-J. Shang, and X.-J. Zhao, Physica A **391**, 5739 (2012).
[6] A. Y. Morozov, Physica A **392**, 2442 (2013).
[7] P. Jizba and J. Korbel, Physica A **413**, 438 (2014).
[8] J.-J. Huang and P.-J. Shang, Physica A **420**, 221 (2015).
[9] H. E. Stanley, L. A. N. Amaral, P. Gopikrishnan, P. Ch. Ivanov, T. H. Keitt, and V. Plerou, Physica A **281**, 60 (2000).
[10] D. Sornette, Phys. Rep. **378**, 1 (2003).
[11] R. Friedrich, J. Peinke, M. Sahimi, and M. R. R. Tabar, Phys. Rep. **506**, 87 (2011).
[12] J. Kwapień and S. Drożdż, Phys. Rep. **515**, 115 (2012).
[13] A. Fisher, L. Calvet, and B. Mandelbrot, Cowles Foundation Discussion Paper 1166 (1997), http://cowles.yale.edu/sites/default/files/files/pub/d11/d1166.pdf.
[14] K. Matia, Y. Ashkenazy, and H. E. Stanley, Europhys. Lett. **61**, 422 (2003).
[15] A. Bershadskii, Physica A **317**, 591 (2003).
[16] T. Di. Matteo, T. Aste, and M. M. Dacorogna, Physica A **324**, 183 (2003).
[17] P. C. Oświe, J. Kwapień, and S. Drożdż, Physica A **347**, 626 (2005).
[18] Z. Eisler and J. Kertész, Eur. Phys. J. B **51**, 145 (2006).
[19] Z. Eisler and J. Kertész, Europhys. Lett. **77**, 29001 (2007).
[20] F. Ren and W.-X. Zhou, Europhys. Lett. **84**, 68001 (2008).
[21] F. Wang, K. Yamasaki, S. Havlin, and H. E. Stanley, Phys. Rev. E **77**, 016109 (2008).
[22] F. Wang, K. Yamasaki, S. Havlin, and H. E. Stanley, Phys. Rev. E **79**, 016103 (2009).
[23] W.-X. Zhou and D. Sornette, Physica A **388**, 2623 (2009).
[24] Z.-Q. Jiang, W. Chen, and W.-X. Zhou, Physica A **388**, 433 (2009).
[25] G. Oh, C. Eom, S. Havlin, W.-S. Jung, F. Wang, H. E. Stanley, and S. Kim, Eur. Phys. J. B **85**, 214 (2012).
[26] D. Stošić, D. Stošić, T. Stošić, and H. E. Stanley, Physica A **428**, 13 (2015).
[27] D. Stošić, D. Stošić, T. Stošić, and H. E. Stanley, Physica A **428**, 46 (2015).
[28] E. E Peters, *Fractal Market Analysis: Applying Chaos Theory to Investment and Economics* (Wiley & Sons, New York, 1994).
[29] P. Ch. Ivanov, L. A. N. Amaral, A. L. Goldberger, S. Havlin, M. G. Rosenblum, Z. Struzik, and H. E. Stanley, Nature **399**, 461 (1999).
[30] P. Ch. Ivanov, A. Bunde, L. A. N. Amaral, S. Havlin, J. Fritsch-Yelle, R. M. Baevsky, H. E. Stanley, and A. L. Goldberger, Europhys. Lett. **48**, 594 (1999).
[31] H. E. Stanley, L. A. N. Amaral, A. L. Goldberger, S. Havlin, P. Ch. Ivanov, and C.-K. Peng, Physica A **270**, 309 (1999).
[32] L. A. Nunes Amaral, P. C. Ivanov, N. Aoyagi, I. Hidaka, S. Tomono, A. L. Goldberger, H. E. Stanley, and Y. Yamamoto, Phys. Rev. Lett. **86**, 6026 (2001).
[33] P. Ch. Ivanov, L. A. N. Amaral, A. L. Goldberger, S. Havlin, M. G. Rosenblum, H. E. Stanley, and Z. Struzik, Chaos **11**, 641 (2001).
[34] P. Ch. Ivanov, A. L. Goldberger, and H. E. Stanley, in *Fractal and Multifractal Approaches in Physiology, in Science of Disaster: Market Crashes, Heart Attacks, and Climate Disruptions*, edited by A. Bunde, J. Kropp, and H. J. Schellnhuber (Springer, Berlin, 2002).
[35] A. L. Goldberger, L. A. N. Amaral, J. M. Hausdorff, P. Ch. Ivanov, C.-K. Peng, and H. E. Stanley, Proc. Natl. Acad. Sci. U.S.A. **99**, 2466 (2002).
[36] C. Thamrin, G. Stern, and U. Frey, Paediatr. Respir. Rev. **11**, 123 (2010).
[37] P. Duarte-Neto, B. Stošić, T. Stošić, R. Lessa, M. V. Milošević, and H. E. Stanley, PLoS ONE **9**, e115262 (2014).
[38] C. Gu, C. P. Coomans, K. Hu, F. A. J. L. Scheer, H. E. Stanley, and J. H. Meijer, Proc. Natl. Acad. Sci. U.S.A. **112**, 2320 (2015).
[39] C.-K. Peng, S. V. Buldyrev, A. L. Goldberger, S. Havlin, F. Sciortino, M. Simons, and H. E. Stanley, Nature **356**, 168 (1992).
[40] B. Hao, H. C. Lee, and S. Zhang, Chaos Solitons Fractals **11**, 825 (2000).
[41] H. Yang, F. Zhao, Y. Zhuo, X. Wu, and Zhuxia Li, Phys. Lett. A **292**, 349 (2002).
[42] A.-B. Guenter, Gene **498**, 20 (2012).
[43] M. S. Roulston, Physica D **125**, 285 (1999).
[44] R. Oliver and J. L. Ballester, Phys. Rev. E **58**, 5650 (1998).
[45] A. Eke, P. Herman, J. B. Bassingthwaighte, G. M. Raymond, D. Percival *et al.*, Pflug. Arch. Eur. J. Physiol. **439**, 403 (2000).
[46] A. Eke, P. Herman, L. Kocsis, and L. R. Kozak, Physiol. Meas. **23**, R1 (2002).
[47] S. Katsev and I. L. Heureux, Comput. Geosci. **29**, 1085 (2003); J. C. R. Pacheco and D. T. Roman, "What is the required series length for correct self-similarity analysis?" https://www.researchgate.net/publication/268178465_What_Is_The_Required_Series_Length_For_Correct_Self-Similarity_Analysis.
[48] M. Kirchner, P. Schubert, D. Schmidtbleicher, and C. T. Haas, Physica A **391**, 4692 (2012).
[49] D. Delignieres, S. Ramdani, L. Lemoine, K. Torre, M. Fortes *et al.*, J. Math. Psychol. **50**, 525 (2006).
[50] J. W. Kantelhardt, E. Koscielny-Bunde, D. Rybski, P. Braun, A. Bunde, and S. Havlin, J. Geophys. Res. **111**, D01106 (2005).
[51] C.-K. Peng, S. V. Buldyrev, S. Havlin, M. Simons, H. E. Stanley, and A. L. Goldberger, Phys. Rev. E **49**, 1685 (1994).
[52] K. Hu, P. Ch. Ivanov, Z. Chen, P. Carpena, and H. E. Stanley, Phys. Rev. E **64**, 011114 (2001).
[53] H. E. Stanley, J. W. Kantelhardt, S. A. Zschiegner, E. Koscielny-Bunde, S. Havlin, and A. Bunde, Physica A **316**, 87 (2002).
[54] B. Podobnik and H. E. Stanley, Phys. Rev. Lett. **100**, 084102 (2008).
[55] B. Podobnik, D. Horvatic, A. M. Petersen, and H. E. Stanley, Proc. Natl. Acad. Sci. U.S.A. **106**, 22079 (2009).
[56] H. E. Hurst, Trans. Am. Soc. Civil Eng. **116**, 770 (1951); A. W. Lo, Econometrica **59**, 1279 (1991).
[57] J. A. Bonachela, H. Hinrichsen, and M. A. Munoz, J. Phys. A: Math. Theor. **41**, 202001 (2008).

[58] N. Scafetta, *Fractal and Diffusion Entropy Analysis of Time Series: Theory, Concepts, Applications and Computer Codes for Studying Fractal Noises and Lévy Walk Signals* (Omniscriptum Publishing Group, Saarbrücken, Germany, 2010).
[59] P. Grigolini, D. Leddon, and N. Scafetta, Phys. Rev. E **65**, 046203 (2002).
[60] N. Scafetta and B. J. West, Phys. Rev. Lett. **90**, 248701 (2003).
[61] N. Scafetta, P. Grigolini, T. Imholt, J. Roberts, and B. J. West, Phys. Rev. E **69**, 026303 (2004).
[62] N. Scafetta and B. J. West, Physics Today **62**(11), 8 (2009); Phys. Rev. Lett. **105**, 219801 (2010).
[63] H. Yang, F. Zhao, L. Qi, and B. Hu, Phys. Rev. E **69**, 066104 (2004).
[64] H. Yang, F. Zhao, W. Zhang, and Z. Li, Physica A **347**, 704 (2005).
[65] S. Cai, P. Zhou, H. Yang, C. Yang, B. Wang, and T. Zhou, Physica A **367**, 337 (2006).
[66] N. Scafetta, R. Moon, and B. J. West, Complexity **12**, 12 (2007).
[67] S. Cai, P. Zhou, H. Yang, T. Zhou, B. Wang, and F. Zhao, Physica A **375**, 687 (2007).
[68] N. Scafetta, D. Marchi, and B. J. West, Chaos **19**, 026108 (2009).
[69] C. Acquisti, P. Allegrini, P. Bogani, M. Buiatti, E. Catanese, L. Fronzoni, P. Grigolini, G. Mersi, and L. Palatella, Chaos Solitons Fractals **20**, 127 (2004).
[70] F. Zhao, H. Yang, and B. Wang, J. Theor. Biol. **247**, 645 (2007).
[71] N. Scafetta and B. J. West, Phys. Rev. Lett. **92**, 138501 (2004).
[72] N. Scafetta and B. J. West, Complexity **10**, 51 (2005).
[73] C.-Y. Tsai and C.-F. Shieh, Physica A **387**, 5561 (2008).
[74] J. Perello, M. Montero, L. Palatella, I. Simonsen, and J. Masoliver, J. Stat. Mech.: Theor. Exper. (2006) P11011.
[75] J. Qi and H. Yang, Phys. Rev. E **84**, 066114 (2011).
[76] W. Zhang, L. Qiu, Q. Xiao, H. Yang, Q. Zhang, and J. Wang, Phys. Rev. E **86**, 056107 (2012).
[77] X. Pan, L. Hou, M. Stephen, and H. Yang, Phys. Lett. A **378**, 2591 (2014).
[78] X. Pan, L. Hou, M. Stephen, H. Yang, and C. Zhu, PLOS ONE **9**, e116128 (2014).
[79] A. Bialas and R. Peschanski, Nucl. Phys. B **273**, 703 (1986).
[80] A. Bialas and R. Peschanski, Nucl. Phys. B **308**, 857 (1988).
[81] P. Bozek, M. Poszajczak, and R. Botet, Phys. Rep. **252**, 101 (1995).
[82] I. M. Dremin and J. W. Gary, Phys. Rep. **349**, 301 (2001).
[83] D. Seibert, Phys. Rev. D **41**, 3381 (1990).
[84] H. C. Eggers, P. Carruthers, P. Lipa, and I. Sarcevic, Phys. Rev. D **44**, 1975 (1991).
[85] X. Cai, C. B. Yang, and Z. M. Zhou, Phys. Rev. C **54**, 2775 (1996).
[86] H. Yang, F. Zhao, Y. Zhuo, X. Wu, and Z. Li, Physica A **312**, 23 (2002).
[87] A. Bialas, Phys. Rev. C **75**, 024904 (2007).
[88] D. Kambly, C. Flindt, and M. Buttiker, Phys. Rev. B **83**, 075432 (2011).
[89] A. K. Mohanty and A. V. S. S. Narayana Rao, Phys. Rev. Lett. **84**, 1832 (2000).
[90] P. Bernaola-Galvan and P. Carpena, Phys. Rev. Lett. **88**, 219803 (2002).
[91] Z.-Q. Ouyang, C. Wang, and Z.-S. She, Phys. Rev. Lett. **93**, 078103 (2004).
[92] F. Zhao, H. Yang, and B. Wang, Phys. Rev. E **72**, 046119 (2005).
[93] R. C. Hwa, Phys. Rev. D **51**, 3323 (1995).
[94] S.-S. Wang, J. Zhang, Y.-X. Ye, and C.-G. Xiao, High Energ. Phys. Nuc. **9**, 769 (1997), in Chinese.
[95] C. Tsallis, J. Stat. Phys. **52**, 479 (1988).
[96] C. Tsallis, *Introduction to Nonextensive Statistical Mechanics: Approaching a Complex World* (Springer, New York, 2009).
[97] V. Garcia-Morales and K. Krischer, Proc. Natl. Acad. Sci. U.S.A. **108**, 19535 (2011).
[98] C. R. S. Banerji, S. Severini, and A. E. Teschendorff, Phys. Rev. E **87**, 052814 (2013).
[99] L. Barnett and A. K. Seth, Phys. Rev. E **91**, 040101(R) (2015).
[100] P. Grassberger, Phys. Lett. A **97**, 227 (1983).
[101] H. G. E. Hentschel and I. Procaccia, Physica D **8**, 435 (1983).
[102] R. A. Brualdi, *Introductory Combinatorics*, 5th ed. (Pearson Education Asia Limited and China Machine Press, Beijing, China, 2009), pp. 281–291.
[103] M. J. D. Powell, *Approximation Theory and Methods* (Cambridge University Press, Cambridge, 1981).
[104] C. R. Rao and H. Toutenburg, *Linear Models: Least Squares and Alternatives, Springer Series in Statistics*, 3rd ed. (Springer, Berlin, 2008).
[105] G.-F. Gu and W.-X. Zhou, Phys. Rev. E **74**, 061104 (2006).
[106] W.-X. Zhou, Phys. Rev. E **77**, 066211 (2008).
[107] G.-F. Gu, and W. X. Zhou, Phys. Rev. E **82**, 011136 (2010).
[108] Z.-Q. Jiang and W.-X. Zhou, Phys. Rev. E **84**, 016106 (2011).
[109] J. F. Muzy, E. Bacry, and A. Arneodo, Phys. Rev. Lett. **67**, 3515 (1991).
[110] S. Mallat and W. L. Hwang, IEEE Trans. Inf. Theory **38**, 617 (1992).
[111] J. F. Muzy, E. Bacry, and A. Arneodo, Phys. Rev. E **47**, 875 (1993).
[112] J. M. Hausdorff, P. L. Purdon, C.-K. Peng, Z. Ladin, J. Y. Wei, and A.-L. Goldberger, J. Appl. Physiol. **80**, 1448 (1996).
[113] The records are downloaded from the website, http://www.physionet.org/physiobank/database/umwdb/.
[114] http://en.wikipedia.org/wiki/Shanghai_Stock_Exchange.
[115] J. Li, J. Liaoning Shihua Univ. **28**, 89 (2008), in Chinese.